caesar preprint

Specimen shape influence on hysteretic response of bulk ferromagnets

Martin Kružík and Tomáš Roubíček

Document info:

Type:	Preprint
Group:	caesar-smm
Preprint ID:	18
Date:	19.02.2002

this page intentionally left blank

Specimen shape influence on hysteretic response of bulk ferromagnets ⋆

M. Kružík [a,c,*], T. Roubíček [b,c,1]

[a] *CAESAR, Friedensplatz 16, D-53 111 Bonn, Germany*

[b] *Faculty of Mathematics and Physics, Charles University, Sokolovská 83, CZ-186 75 Praha 8, Czech Republic*

[c] *ÚTIA, Academy of Sciences, Pod vodárenskou věží 4, CZ-182 08 Praha 8, Czech Republic.*

Abstract

Influence of shape of a specimen is questioned by computational modeling. A new mesoscopical-level model modifying the conventional micromagnetics in a suitable way is used. Numerical simulations made for uniaxial ferromagnets as, e.g., CoZrDy demonstrate explicit dependence of the hysteretic response on the geometry of the specimen. In particular, it is shown how non-ellipsoidal shape of the specimen causes the main hysteresis loop to be round. Yet, it cannot directly cause appearance of minor hysteretic loops which reflect purely material properties itself, e.g. some fuzziness in the coercive force, as also demonstrated.

Key words: micromagnetism, maximal dissipation, hysteresis, simulation
PACS: 75.40Mg

⋆ Fruitful discussions with dr. Alfred Ludwig, dr. Eckhard Quandt (both `caesar` Stiftung, Bonn) and dr. Ivan Tomáš (Institut of Physics, Prague) are acknowledged. This work was partly supported by the grants 201/00/0768 (GA ČR), A 107 5005 (GA AV ČR), and MSM 11320007 (MŠMT ČR).

* Corresponding author: e-mail: `kruzik@caesar.de`, fax: 0049-(0)228-9656111, phone: 0049-(0)228-9656234

[1] This author acknowledges the support of `caesar`-Stiftung during his stay at this institution in Bonn.

1 Introduction

We pursue a two-fold goal. First, we want to demonstrate how shape of a bulk ferromagnet explicitly influences the hysteretic response. To do this, we follow the second goal by introducing a suitable model which handles the anisotropy of the magnet like in conventional Landau-Lifshitz' micromagnetical model but, because of bulk situation, suppresses the exchange energy contribution and describes the microstructure only on a "mesoscopical" level. This enables us practical computational modeling of "macroscopically" spatial inhomogeneities of magnetization. This inhomogeneity is responsible for roundness of observed main hysteresis loops but, rather surprisingly, cannot cause any minor hysteresis loops in M/H-diagrams if only a single activation threshold (i.e. the coercive field) is considered in the model. It seems that our model allows for these minor loops only if a multi-threshold response of the ferromagnetic material is assumed.

These effects are basically not surprising (cf., e.g., the work by Würschmidt [43] from 1925) but no explicit and, to a good extent, accurate study seems to be performed so far. The exception is for specimens of an ellipsoidal shape magnetized in a homogeneous external magnetic field H parallel to some axis where the *demagnetization field* $H_{\rm d}$ as well a *"macroscopical" magnetization* M remain homogeneous and then $H_{\rm d} = NM/\mu_0$ where μ_0 is the vacuum permeability and N is the so-called *demagnetizing factor* which can be calculated even analytically (as, in general, a diagonal tensor), see Osborn [28] or also, e.g., [13, Sect.3.2.5]. In non-ellipsoidal shapes, the demagnetizing factors can approximately be calculated in special cases (see, e.g., Aharoni [1], Chikazumi [7, Sect.2.2] or O'Handley [27, Sect.2.3]) but under a simplifying assumptions, typically that M is spatially homogeneous. Such considerations, however, ignore complex interactions of the demagnetizing field with the magnetization evolving not homogeneously at particular points of the magnet. This evolution of $M = M(x,t)$ is an activated transformation process with a characteristic activation threshold (cf. (15) below) and depends reciprocally on the resulting magnetic field.

Thus it should be emphasized that, for a general shape and general magnetization regimes, one must rely only on experimental measurements or numerical simulations. The latter option, we are focused on in this paper, seems however difficult to be obtained by conventionally used models which either treat the microstructure in too much detail (so that the multi-level character of macroscopical/microsopical effects cannot be properly modeled because of capacity of usual computers) or replaces the important information about the microstructure by mere phenomenology and smears thus out the complex interrelations counting macroscopical geometry of a specimen. The former sort of (domain-like) models includes Gilbert-Landau-Lifshitz' one [11,21], while

the later one involves, e.g., models based on Rayleigh's modification [32] of Prandtl's and Ishlinskiĭ's model or Preisach's model [30] (see also Jiles [15], Mayergoyz [25], or Visintin [40]). Another one is, e.g., due to Jiles and Atherton [17] and its modifications as, e.g., [16,19].

It can roughly be said that, in the model used here, we combine the so-called *dry-friction* idea with the mesoscopical-level description of microstructure by using basically volume fractions (expressed through Young's [39] parameterized probability measures). In fact, the notion of "dry-friction" is related to the maximum-dissipation principle used routinely in (quasi)plasticity, as mentioned in Section 2.3 more in detail. Let us also mention that the dry-friction is very natural in the context of ferromagnetism, and has been already used in a Jiles-Atherton-like model by Bergqvist [3], in a micromagnetical-type model and in a model based on macroscopical magnetization M (cf. (6)) by Visintin in [41] and [42], respectively. The mesoscopical description of the magnetization has been used by DeSimone [9], James and Kinderlehrer [14], and Rogers [33] (see also [18]) but in a mere Gibbs-energy minimization framework only.

Let us remark that shape influence has, in fact, been investigated computationally already in occasions other than bulk ferromagnets by other models; e.g. for a single nanowire versus array of (20 000 of) nanowires see Raposo at al. [31] or for a multilayered media see Schrefl [38].

A mesoscopical-level evolution model in ferromagnetism has been proposed also in [33] (see also [18]) but no rate-independent dissipation has been involved and the hysteretic response has been obtained by adding a rather nonstandard nonconvex nonlocal term into the steady-state energy $\bar{E}$.

2 The mesoscopical-level model

We briefly introduce the mathematical model which can capture the shape influence as outlined above. For a rigorous mathematical analysis of this model (involving still a certain regularizing term) we refer to [36] while its anisothermal extension has been outlined in [35].

2.1 Stored energy

In the classical "microscopical" theory of rigid ferromagnetic bodies as presented by Brown [4–6], based mainly on works of Landau and Lifshitz [21], the state is described by a *"microscopical" magnetization* $m : \Omega \to \mathbb{R}^3$ depending on a position $x \in \Omega$, where $\Omega \subset \mathbb{R}^3$ denotes a fixed domain (i.e. the body)

occupied by a homogeneous ferromagnetic material. A usual *Heisenberg-Weiss constraint*, i.e.

$$|m(x)| = M_{\rm s} \ , \tag{1}$$

is considered, where $M_{\rm s}$ is the *saturation magnetization* at a fixed temperature (assumed below Curie's point). In the so-called no-exchange formulation which is well acceptable for large ferromagnets (where an exchange energy contribution is indeed negligible, cf. DeSimone [9]) the overall stored energy E consists of two parts:

$$E(m) = \int\limits_{\Omega} \varphi(m(x)) \ \mathrm{d}x + \frac{1}{2} \int\limits_{\mathbb{R}^3} |\nabla u_m(x)|^2 \ \mathrm{d}x, \tag{2}$$

where $u_m : \Omega \to \mathbb{R}$ is a potential of an induced magnetic field. The first term in (2) is an *anisotropy energy* with a density φ which is an even nonnegative function depending on material properties and exhibiting crystallographic symmetry. The second term in (2) is a *magnetostatic energy* coupled with the magnetization field through the equation

$$\mathrm{div}(-\mu_0 \nabla u_m + m\chi_\Omega) = 0, \tag{3}$$

where μ_0 is the vacuum permeability and $\chi_\Omega : \mathbb{R}^3 \to \{0, 1\}$ is the characteristic function of Ω, i.e. $\chi_\Omega(x) = 1$ if $x \in \Omega$ while $\chi_\Omega(x) = 0$ if $x \notin \Omega$. This equation stems from the Maxwell equations

$$\mathrm{div}\ B = 0 \ \ , \ \mathrm{curl}\ H_{\rm d} = 0 \ , \tag{4}$$

where B is the magnetic induction and $H_{\rm d}$ the demagnetization field. By the usual constitutive relation, it holds $B = \mu_0 H_{\rm d} + m$ and, in the special potential case (4), $H_{\rm d} = -\nabla u_m$ for some potential u_m. The equation (3) for u_m then follows immediately.

Then, the *Gibbs free energy* (for a fixed temperature) is

$$G(m) = E(m) - \int\limits_{\Omega} H(x) \cdot m(x) \ \mathrm{d}x \tag{5}$$

where $H : \mathbb{R}^3 \to \mathbb{R}^3$ is an applied *external magnetic field*. The second term in (5) is called an *interaction energy*.

2.2 Mesoscopical description of magnetization

The steady state of a soft ferromagnetic material in the external magnetic field can be described as a minimum of the free energy G from (5). However, in case of (2), the minimizing configuration m may not exist, as shown in [14] for $H = 0$. This nonexistence comes from the competition of the anisotropy energy preferring the magnetization of the constant length and the self-induced field energy preferring to be zero. This (quite generic) non-attainment is caused by the fact that the development of finer and finer self-similar structure decreases the energy but keeps the average "macroscopic" magnetization constant. Hence, we can look at how a given macroscopic magnetization M, which does not have necessarily the given magnitude $M_{\rm s}$, can be obtained from a combination of fine structure magnetizations.

To do this, it is useful to collect a certain information about the fine structure "around" a current point $x \in \Omega$ in the form of a *probability measure*, denoted by ν_x, supported on the sphere S^2 in $\mathbb{R}^3$ of the radius $M_{\rm s}$. Hence we write $\nu_x \in \mathrm{M}_0^+(S^2)$, the set of all probability measures on S^2. Let us furthermore denote the ball in $\mathbb{R}^3$ of the radius $M_{\rm s}$ by B^3. The collection $\nu = \{\nu_x\}_{x\in\Omega}$ is often called a Young measure [39] and can be considered as a certain "mesoscopical" description of the magnetization. The macroscopical magnetization at a material point $x \in \Omega$ is then its first momentum, i.e.

$$M(x) = \int_{S^2} m \; \nu_x(\,\mathrm{d}m) \; . \tag{6}$$

Note that the macroscopical magnetization $M : \Omega \to B^3 \subset \mathbb{R}^3$ "forgets" a detailed information about microstructure in contrast with the mesoscopical magnetization $\nu : \Omega \to \mathrm{M}_0^+(S^2)$ which can capture *volume fraction* related with particular directions of magnetization. It should be emphasized that, though we speak about (collections of) probability measures, our approach is *purely deterministic* (not probabilistic).

On the mesoscopical level, it is then natural to consider the stored energy $\bar{E}$ and the free energy $\bar{G}$ respectively as

$$\bar{E}(\nu) = \int_\Omega \int_{S^2} \varphi(m)\nu_x(\,\mathrm{d}m)\,\mathrm{d}x + \frac{1}{2}\int_{\mathbb{R}^3} |\nabla u_M(x)|^2 \,\mathrm{d}x, \tag{7}$$

$$\bar{G}(\nu) = \bar{E}(\nu) - \int_\Omega H(x)\cdot M(x)\,\mathrm{d}x \; , \tag{8}$$

where $M = M(\nu)$ according to (6) and u_M is determined by

$$\mathrm{div}(-\mu_0 \nabla u_M + M\chi_\Omega) = 0 \ . \tag{9}$$

An interesting property of both $\bar{E}$ and $\bar{G}$ is that they are convex with respect to the natural geometry of the considered parameterized probability measures ν's, let us denote this (also convex) set as $\mathrm{Y}(\Omega; S^2)$, and that the minimum of $\bar{G}$ on $\mathrm{Y}(\Omega; S^2)$ is indeed attained. The mesoscopical steady-state configuration ν minimizing $\bar{G}$ describes how "to organize" the fine scale structure (microstructure) in order to get the right macroscopic behavior. We refer to [9,14,29,33] for mathematically rigorous reasoning and for relation between the microscopical and mesoscopical steady-state energy-minimization problems.

2.3 Evolution, rate-independent dissipation

Minimization of the free energy (8) can model a steady state or also quasi-stationary evolution under low-frequency applied field $H = H(t)$ of soft magnetic materials with a reasonable accuracy. Varying the applied external magnetic field H then does not produce any hysteresis on M/H-diagram. On the other hand, magnetically hard materials exhibit significant hysteresis and thus cannot be modeled by mere minimization of the free energy $\bar{G}$. Let us remind that $\bar{G}$ is convex so it does not have any local minima, but even if a minimization of the "microscopical" nonconvex free energy G (possibly with an exchange-energy term) would be considered, some hysteresis can result but it cannot be controlled by an independent parameter which may lead to incorrect numerical effects, cf. [31] where a coercive field for cobalt resulted as 900 Oe instead of an experimentally observed (see [7, p.19]) value 10 Oe.

As the hysteretic response is rate-independent at least for H varying not with extremely high-frequencies, we can be inspired by plasticity theory where so-called Hill's [12] *maximum-dissipation* principle typically governs activated processes arising there. This involves Rayleigh's *dissipation potential* R which is necessarily convex, non-negative and positively homogeneous. Its subdifferential, denoted by $\partial R(\nu) = \{\omega;\ \forall \tilde{\nu} :\ R(\tilde{\nu}) \geq R(\nu) + \langle \omega, \tilde{\nu} - \nu \rangle\}$, is a so-called maximal responsive set-valued map, see Eve, Reddy, and Rockafellar [10] for a deep investigation. The desired evolution $\nu = \nu(t)$ is then governed by a simple first-order differential inclusion

$$\partial R(\frac{\mathrm{d}\nu}{\mathrm{d}t}) + \partial \bar{E}(\nu) \ni \bar{H}(t) \tag{10}$$

with an initial condition $\nu|_{t=0} = \nu^0$, where $\partial \bar{E}$ denotes the subdifferential of $\bar{E}$ (considered as extended on the whole space of parameterized measures $L^\infty_{\mathrm{w}}(\Omega; M(S^2))$ by $\bar{E}(\nu) = +\infty$ if $\nu \notin \mathrm{Y}(\Omega; S^2)$, see [36] for more details)

and $\bar{H} = \bar{H}(t)$ stands for the linear functional related in a natural way with $H = H(t)$ by the formula $\nu \mapsto \int_\Omega H(t) \cdot M \ \mathrm{d}x$ with $M = M(\nu)$ depending linearly on ν through (6).

Obviously, (10) can be written as

$$\omega + \partial\bar{E}(\nu) \ni \bar{H}(t), \quad \omega \in \partial R(\,\mathrm{d}\nu/\,\mathrm{d}t). \tag{11}$$

As the subdifferential ∂R is assumed maximal responsive, by [10, Lemma 4.1(c,d)] the latter inclusion in (11) is equivalent to

$$\langle \frac{\mathrm{d}\nu}{\mathrm{d}t}, \omega \rangle = \max_{\tilde{\omega} \in \mathfrak{C}} \langle \frac{\mathrm{d}\nu}{\mathrm{d}t}, \tilde{\omega} \rangle \tag{12}$$

where the convex set $\mathfrak{C} = \partial R(0) = \{\omega;\ \forall \nu :\ \langle \omega, \nu \rangle \leq R(\nu)\}$ determines the region of nondissipative (i.e. nonhysteretic) response. The relation (12) is just what is called the maximum dissipation principle, and expresses the rule that the rate of change of microstructure ν is normal to $\mathfrak{C}$ at ω.

The potential $R = R(\dot{\nu})$ is to describe *phenomenologically* all dissipative mechanisms observed on the mesoscopical level. This enables us not to have to deal with all details connected with complicated domain evolution on the microscopical level and to model it in a simplified but effective way only bearing in mind an experimentally observed macroscopical energetics. Besides a form of φ, this represents the only phenomenology built in our model. It is especially simple for *uniaxial magnets* where we should basically only set up the energy, denoted by $\mathfrak{D}$ (cf. (19) below), needed for (or, in other words, dissipated by) the transformation of the magnetization from one pole to the other or vice versa. This effect can be obtained by choosing

$$R(\nu) = \int_\Omega \left| \int_{S^2} \lambda(m) \nu_x(\,\mathrm{d}m) \right| \mathrm{d}x \tag{13}$$

with $\lambda : S^2 \to \mathbb{R}$ being constant near each poles. Considering the unit vector $e_3 = (0, 0, 1)$ as the easy-magnetization axis, the poles will be at $m = \pm M_\mathrm{s} e_3$. For a dominant anisotropy, one can assume that the magnetization will be mostly in a close vicinity of the poles, i.e. $m \sim \pm M_\mathrm{s} e_3$, and then the landscape of λ out of the poles is nearly insignificant. Hence one can simply take λ linear:

$$\lambda(m) = H_\mathrm{c}\, m \cdot e_3 \equiv H_\mathrm{c} m_3 \tag{14}$$

with the scalar parameter H_c having the meaning of the *coercive field* considered as fixed, i.e. no "isotropic hardening" effects (like in [2]) that could

model a virgin magnetization curve are considered. In particular, no dissipation (or, equivalently, no activation threshold) appears for changing m_1 or m_2 components of the magnetization vector $m = (m_1, m_2, m_3)$, which agrees with experimental observations for uniaxial ferromagnetical single-crystals. Thus λ basically indicates whether the magnetization lives around the particular pole $m \sim \pm M_s e_3$ according to approaching the scalar value $\lambda(m) \sim \pm H_c M_s$. As such, λ can be understood as a certain *pole indicator*, playing the role what is often called the "order parameter". Note that, due to (6) and (14), we now have $R(\nu) = \int_\Omega H_c |M_3(x)| \, \mathrm{d}x$.

By analyzing the abstract maximum-dissipation principle (12) for the special case (13)–(14), one can identify the point-wise explicit activation rule that triggers the magnetization evolution process:

$$\frac{\mathrm{d}M_3}{\mathrm{d}t} \begin{cases} = 0 \Longleftarrow -H_c < \mathfrak{H} < H_c, \\ > 0 \Longrightarrow \mathfrak{H} = H_c, \\ < 0 \Longrightarrow \mathfrak{H} = -H_c. \end{cases} \tag{15}$$

cf. [36, Formula (5.13)]. Moreover, the first inclusion in (11) says, after a detailed analysis, that the scalar function $\mathfrak{H} = \mathfrak{H}(x,t)$ appearing in (15), which plays a role of an *effective field* which activates the magnetization process, satisfies

$$\mathfrak{H}(x,t) \in H_c \mathrm{sign}(M_3), \tag{16}$$

where $\mathrm{sign}(M_3)$ denotes the multivalued function being equal to 1 (resp. -1) for M_3 positive (resp. negative) and to the interval [-1,1] for $M_3 = 0$. In addition, the probability measure $\nu_{x,t}$ describing "mesoscopically" magnetization at a point $x \in \Omega$ and time t must be supported only at those points $s \in S^2$ where the function

$$m \mapsto \varphi(m) + \mathfrak{H} m_3 + (H_d - H) \cdot m \tag{17}$$

is minimized, cf. [36, Formulae (5.4g) and (5.6)].

Though the behavior controlled by (15)–(17) might not be convincing, the main theoretical justification of the model relies on the energy balance. This can be got by testing (10) by the rate of mesoscopical magnetization $\mathrm{d}\nu/\mathrm{d}t$ and integrating it over a considered time interval $[t_1, t_2]$. This gives

$$\bar{E}(\nu(t_2)) - \bar{E}(\nu(t_1)) + H_c \int_\Omega \operatorname*{Var}_{t_1 \le t \le t_2} M_3(x,t) \, \mathrm{d}x$$

$$= \int_{t_1}^{t_2} \int_{\Omega} H(t) \cdot \frac{\partial M}{\partial t} \, \mathrm{d}x \, \mathrm{d}t, \tag{18}$$

where the symbol "Var" denotes the total variation over the interval $[t_1, t_2]$ indicated below it. Therefore this term basically counts, roughly speaking, how many times the magnetization was reversed between the two poles during the time interval $[t_1, t_2]$ at a current point $x \in \Omega$, independently of how fast the transformation process was. Hence (18) says that the difference between the stored energies at the final time $t = t_2$ and at the initial time $t = t_1$ plus the total energy dissipated during the pole transformations over the interval $[t_1, t_2]$ at each point $x \in \Omega$ equals to the work done by the external magnetic field H. This also determines the area of the main hysteresis loop in the M/H-diagram which must be exactly $4M_{\mathrm{s}}H_{\mathrm{c}}$ provided the magnetization after completing the magnetization process lies exactly at the pole $M_{\mathrm{s}}e_3$ or $-M_{\mathrm{s}}e_3$. Hence the specific energy needed for transformation of one pole to the other is

$$\mathfrak{D} = 2M_{\mathrm{s}}H_{\mathrm{c}}. \tag{19}$$

It is important that this energy can be chosen as an independent phenomenological parameter (in particular, independently of the landscape of the anisotropy energy φ) which enables us to incorporate all main experimental data into the model. For example, impurities or dislocations in the atomic grid may considerably influence the energy $\mathfrak{D}$ without changing considerably the anisotropy energy φ. Contrary to this phenomenology, the macroscopical interactions taking into the account the geometrical shape of the specimen Ω are treated independently and with a full rigor through (9).

Let us still remark that the situation in cubic magnets having 6 or 8 poles would differ only by a necessity to design the dissipative potential in a more complex way to describe energy needed to activate (or, in other words, dissipated by) various pole transformation processes.

2.4 Numerics and implementation

Though numerical approximation, analysis, and implementation of the model (10) is not the essential point in this paper, we mention only briefly these (otherwise quite important) issues; for more details see [20].

We use implicit time discretization of (10) with a constant time step τ. Denoting ν^k the approximate value of $\nu(t)$ at time $t = k\tau$, we consider the so-called backward Euler scheme:

$$\partial R(\frac{\nu^k - \nu^{k-1}}{\tau}) + \partial \bar{E}(\nu^k) \ni \bar{H}(k\tau) \tag{20}$$

for $k = 1, 2, ...$ recursively. Of course, for $k = 0$, we take ν^0 as the initial condition for (10). Taking into account the convexity of both R and $\bar{E}$, one can calculate the solution ν^k of (20) simply as a minimizer of the convex function

$$\nu \mapsto \bar{E}(\nu) + \tau R(\frac{\nu - \nu^{k-1}}{\tau}) - \langle \bar{H}(k\tau), \nu \rangle \tag{21}$$

on the convex set $\mathrm{Y}(\Omega; S^2)$.

The *finite-element* method (in fact, here rather the finite-volume method) is used to solve the above problem numerically. Taking $d_1 > 0$, the domain Ω is divided into subdomains $\{\Omega_j\}_{j=1}^{N(d_1)}$, called finite elements, with diameter not exceeding d_1. Further, as the Young measure is supported on S^2, for any $d_2 > 0$ we choose $N(d_2)$ different points $\{m^i_{d_2}\}_{i=1}^{N(d_2)}$ on S^2 which make the support of an approximate Young measure $\nu^d = \{\nu^d_x\}$, $d = (d_1, d_2)$. Thus, at a current time level k, ν^d is considered to be constant on each finite element and of the form

$$\nu^d_x = \sum_{i=1}^{N(d_2)} \gamma^i_d(x) \delta_{m^i_{d_2}} \ , \ x \in \Omega \ , \tag{22}$$

where δ_m denotes Dirac's mass supported at $m \in S^2$ and $\gamma^i_d(x) \geq 0$ and $\sum_{i=1}^{N(d_2)} \gamma^i_d(x) = 1$ for all $x \in \Omega$, i.e., γ^i_d are element-wise constant as well.

At a current time level k, in view of (6), the approximate macroscopic magnetization M^d is then given by

$$M^d(x) = \sum_{i=1}^{N(d_2)} \gamma^i_d(x) m^i_{d_2} \ . \tag{23}$$

As the 3-dimensional situation is computationally very demanding, we confine ourselves to axi-symmetrical situations that can be reduced to a two-dimensional problems. Thus the sphere S^2 reduces to a circle S^1. Here, we consider two different cylinders, and a cylinder with two coaxial holes in upper and lower bases which creates an "H-shaped" cross-section, see Figure 1 below. Moreover, all our examples admit a planar symmetry with respect to the horizontal plane $\{x_3 = 0\}$, cf. again Figure 1 below, which enables us to make another reduction of variables. The demagnetizing field ∇u_M from (9) produced by a subdomain Ω_j can be calculated for any $x \in \mathbb{R}^3$ exactly through

$$\nabla u_M(x) = -\frac{1}{\mu_0}\Big(\int\limits_{\Omega_j} \frac{(x-y)\ \mathrm{div}\ M(y)}{|x-y|^3}\,\mathrm{d}y - \int\limits_{\partial\Omega_j} \frac{(x-y)M(y)\cdot n(y)}{|x-y|^3}\,\mathrm{d}y\Big), \tag{24}$$

where n denotes the unit outer normal to the boundary $\partial\Omega_j$ of Ω_j. As we consider the magnetization to be constant within each subdomain Ω_i the first term on the right hand side of (24) vanishes. Eventually, the second term on the right hand side of (24) is evaluated using a numerical quadrature rule, which can be considered as a version of the dipole formula; cf. e.g. [31]. Each subdomain is uniformly copied 18 times by a rotation around x_3 (i.e. each 20 degrees) and magnetization vectors in such a rotated subdomain are considered to be the rotated magnetizations from the original domain.

Although (21) is a nonsmooth problem it can be turned into a smooth linear-quadratic programming problem with some additional linear constraints and auxiliary variables. The circle S^1 has been discretized to $N(d_2) = 8$ points and the number of elements was $N(d_1) = 32$ on one quarter actually calculated. The resulting linear-quadratic program for γ_d^i and auxiliary variables was solved by Schittkowski's NLPQL [37]. We refer to [20,36] for implementation details.

3 Computations of ferromagnets of various shapes

As announced above, we now want to present usage of the above introduced model for investigation of influence of shape of a specimen of a uniaxial ferromagnet on its M/H-response. Simulating real experiment, we must naturally set up three mutually independent data sets: material, geometrical shape of Ω, and the external magnetic field $H = H(x,t)$.

As to the *material data*, to be more specific, let us consider as in [8] a *CoZrDy* homogeneous amorphous alloy (at the temperature 4.2 K) which has indeed uniaxial structure assumed in (13)–(14). Considering again the easy-magnetization axis to be parallel with the unit vector $e_3 = (0,0,1)$, the uniaxial anisotropy energy density is taken as

$$\varphi(m) = K\sin^2\theta \tag{25}$$

with θ the angle between the vectors m and e_3, $K = 40\ \mathrm{kJ/m^3}$ and the saturation magnetization $M_\mathrm{s} = 0.05\,\mathrm{T}$; cf. [8]. Then, considering the dissipative energy (13)–(14), it remains to determine the coercive field H_c; here, we take

$H_c = 20$ MA/m. In accord with (19), this gives the specific pole-transformation energy $\mathfrak{D} = 2$ MJ/m^3.

As to the external magnetic field $H = H(x,t)$, we consider it spatially homogeneous (i.e. independent of $x \in \Omega$) as it is, with high accuracy, often the case in lab experiments. Hence only a *time-dependence of* $H = H(t)$ is to be set up. As the model is rate independent, in fact only a direction and the reached magnitude of H is essential. Up to the (irrelevant) velocity, the used function $H = H(t)$ can thus be easily reconstructed from the presented H/M-diagrams and therefore will not be specified.

Finally, the *geometrical shape* of a specimen varied. All the specimens are axially symmetric with respect to the vertical axis x_3 and symmetric with respect to the horizontal plane $\{x_3 = 0\}$. Figure 1 below shows planar cuts by a plane containing the axis x_3. In all cases, the easy magnetization axis e_3 is vertical, as well as the applied field H, i.e., $H = (0, 0, H_3)$.

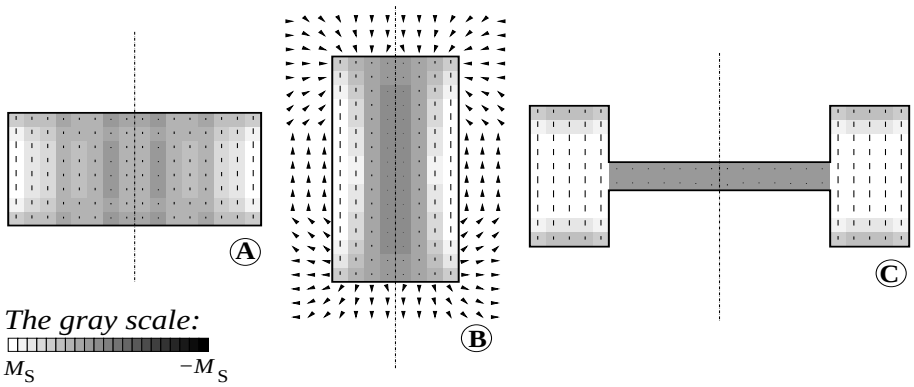

Fig.1: Cross-sections of various specimens with computed inhomogeneous magnetization (and for B also the demagnetizing field around) displayed at specific time instances.

The gray levels correspond to the macroscopical magnetization M_3 (white means $M_3(x) = M_s$ while black is $M_3(x) = -M_s$) at the average magnetization about 23 mT for A and B and at about 35 mT for C on the right-hand branch of the hysteresis loop. We can therefore easily see the nonhomogeneity of the magnetization resulting from an interaction with the self–induced demagnetizing field. Besides, the magnetization vector field $M(x)$ in the magnet Ω and, in case B, also the demagnetizing field $H_d(x)$ outside Ω is displayed by the arrows. The corresponding main hysteresis loops (the spatially averaged component M_3 vs. the H_3 component of the external field) are on Figure 2.

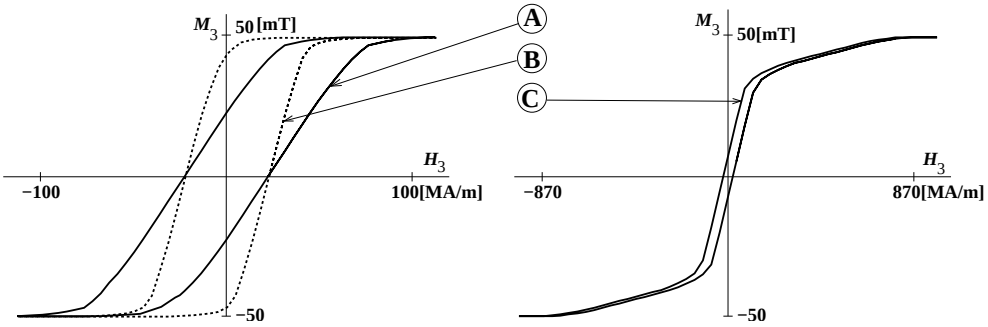

Fig.2: Corresponding hysteresis loops.

We can see that magnetizing a longer magnet (Fig.1b) produces the hysteresis loop more up-righted in comparison with a flat magnet (Fig.1a), which is a well known effect usually described roughly by speaking about a larger demagnetizing factor. In any case, however, it is not possible to produce minor hysteresis loops; more precisely, the minor loops have the zero area and degenerate thus to perfectly horizontal lines.

To produce minor loops, it seems indeed inevitable to consider more than only one activation threshold H_c. We demonstrate this effect simply by imposing a spatial inhomogeneity of the coercive field $H_c = H_c(x)$. E.g. a random variation $\pm 45\%$ of H_c around the previously used value $H_c = 20$ MA/m (i.e. $H_c(x)$ being piece-wise constant and uniformly randomly distributed over the interval $[11, 29]$ MA/m) changes the response from Fig.2 (Case A) as follows:

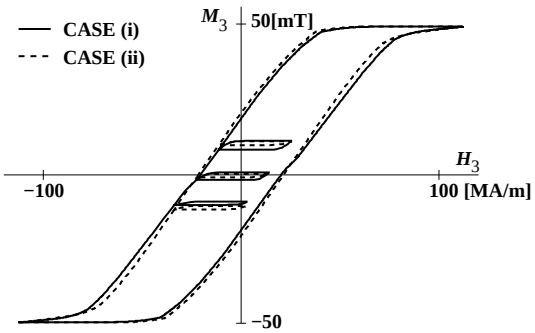

Fig.3: Minor hysteresis loops on the specimen A but with inhomogeneous material having randomly distributed coercive field $H_c = 20(\pm 45\%)$ MA/m.

Two test cases of (pseudo)random distribution of H_c are displayed.

An interesting, but perhaps not entirely surprising effect is that, although $H_c(x)$ is distributed randomly, the resulting macroscopical magnetization $M_3(x)$ is self-organized by collective interactions to vertical stripes, which is obviously to minimize the energy of the created demagnetizing field. This is displayed on the following snapshots corresponding to those test cases at one specific time:

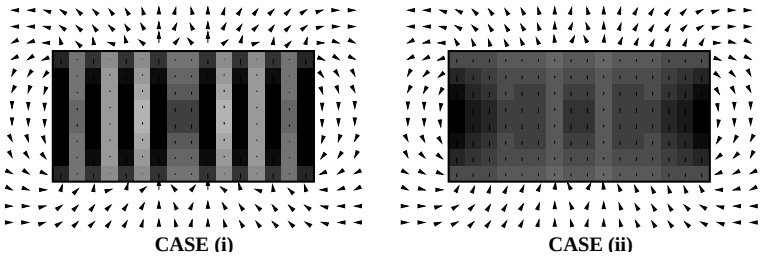

Fig.4: Computed magnetization on the specimen A with the two cases of inhomogeneous material.

4 Concluding remarks

We presented an efficient and rigorous method how to compute demagnetizing-field effects in ferromagnets of arbitrary shape. In particular, we showed very explicitly how main hysteresis loops are made round as a consequence of an non-ellipsoidal shape of the specimen. This effect is additional to the overall averaged inclination of the hysteresis loop which is, of course, also affected by the specimen shape, but this effect was well known even for ellipsoidal-shape bodies through the demagnetizing factor. Moreover, we showed that a suitable shape can thus effectively produce two (or certainly even more) significantly different demagnetizing factors at the single specimen, cf. again Figure 2C.

Moreover, we also showed that minor hysteretic loops cannot be produced, perhaps rather surprisingly, as a mere consequence of the macroscopical geometry but result ultimately from a multi-threshold behavior of the material itself.

The method can be used in a more sophisticated arrangement: relying on the formula (25), one can first fit the material parameters φ, i.e. here K in accord to (25), and $H_{\rm c}$ and $M_{\rm s}$ with an experiment made on a specimen with a specific shape, and then one can predict hysteretic response for other experiments made possibly on specimen of a different shape or under a different magnetization regimes.

References

[1] A. Aharoni, J. Appl. Physics 83 (1998), 3432–3434.

[2] J. Aktaa, A. von der Weth, J. Magnetism & Magn. Mater. 212 (2000), 267–272.

[3] A. Bergqvist, Physica B 233 (1997), 342–347.

[4] W.F. Brown, Jr., Magnetostatic interactions, North-Holland, Amsterdam, 1962.

[5] W.F. Brown, Jr., Micromagnetics, Interscience, New York, 1963.

[6] W.F. Brown, Jr., Magnetostatic principles in ferromagnetism, Springer, New York, 1966.

[7] S. Chikazumi, Physics of Magnetism. J.Wiley, New York, 1964.

[8] O.A. Chubykalo, J.M. Gonzáles, G.R. Aranda, J. Gonzáles, J. Magnetism & Magn. Mater. 222 (2000), 314–326.

[9] A. DeSimone, Arch. Rat. Mech. Anal. 125 (1993), 99–143.

[10] R.A. Eve, B.D. Reddy, R.T. Rockafellar, Quarterly Appl. Math. 48 (1990), 59–83.

[11] T.L. Gilbert, Phys. Rev. 100 (1955), 1243.

[12] R. Hill, Q.J. Mech. Appl. Math. 1 (1948), 18–28.

[13] A. Hubert, R. Schäfer, Magnetic Domains. Springer, Berlin, 1998.

[14] R.D. James, D. Kinderlehrer, Continuum Mech. Thermodyn. 2 (1990), 215–239.

[15] D. Jiles, Introduction to magnetism and magnetic materials. Chapman & Hall, London, 1991.

[16] D. Jiles, IEEE Trans. Mag. 28 (1992), 2603.

[17] D.C. Jiles, D.L. Atherton, J. Magnetism & Magn. Mater. 61 (1986), 48–60.

[18] M.K. Keane, R.C. Rogers, In: Proc. SPIE (Int. Soc. for Optical Engineering) Vol. 2192, 1994, pp. 52-63.

[19] P.I. Koltermann, at al., Physica B 275 (2000), 233-237.

[20] M. Kružík, (Preprint `caesar`, Bonn, no. 8/2001.) ESAIM: M2AN (submitted).

[21] L.D. Landau, E.M. Lifshitz, Physik Z. Sowjetunion 8 (1935), 153–169.

[22] E.M. Lifschitz, J. Phys. USSR 8 (1944), 337–346.

[23] M. Luskin, L. Ma, SIAM J. Numer. Anal. 29 (1992), 320–331.

[24] L. Ma, Ph.D. Thesis, University of Minnesota, Minneapolis. (1991).

[25] I.D. Mayergoyz, Mathematical Models of Hysteresis. Springer, New York, 1991.

[26] A. Mielke, F. Theil, In: Proc. Models of Cont. Mechanics in Analysis and Engineering, Shaker-Verlag, Aachen, 1999, pp. 117–129.

[27] R.C. O'Handley, Modern Magnetic Materials, J.Wiley, New York, 2000.

[28] J.A. Osborn, Phys. Rev. 67 (1945), 351.

[29] P. Pedregal, Parametrized Measures and Variational Principles, Birkhäuser, Basel, 1997.

[30] F. Preisach, Z. Physik 94 (1935), 277-302.

[31] V. Raposo, J.M. Garcia, J.M. Gonzáles, M. Vázquez, J. Magnetism & Magn. Mater. 222 (2000), 227–232.

[32] Lord Rayleigh, Phil. Mag. 23 (1887), 225–248.

[33] R.C. Rogers, J. Integral Eq. Appl. 3 (1991), 85–127.

[34] T. Roubíček, Relaxation in Optimization Theory and Variational Calculus, W. de Gruyter, Berlin, 1997.

[35] T. Roubíček, In: Bexbach Coll. on Sci. (Eds. A.Ruffing, M.Robnik), Shaker Ver., Aachen, in print.

[36] T. Roubíček, M. Kružík, (`caesar` preprint no. 3/2000, Bonn) Zeit. Angew. Math. Physik (accepted).

[37] K. Schittkowski, Annals of Operation Research 5 (1985-6), 485–500.

[38] T. Schrefl, J. Magnetism & Magn. Mater. 207 (1999), 45–65, 66–67.

[39] L.C. Young, Comptes Rendus de la Société et des Lettres de Varsovie, Classe III 30 (1937), 212–234.

[40] A. Visintin, Differential Models of Hysteresis. Springer, Berlin, 1994.

[41] A. Visintin, Physica B 233 (1997), 365–369.

[42] A. Visintin, Physica B 275 (2000), 87–91.

[43] J. Würschmidt, Theorie des Entmagnetisierungsfaktors und der Scherung von Magnetisierungskurven. Vieweg & Sohn, Braunschweig, 1925.